Attenuation Correction Strategies for Positron Emission Tomography/Computed Tomography and 4-Dimensional Positron Emission Tomography/Computed Tomography

Tinsu Pan, PhD[a,*], Habib Zaidi, PhD, PD[b,c,d]

KEYWORDS

• Positron emission tomography/computed tomography • Average computed tomography
• 4-dimensional computed tomography • 4-dimensinal positron emission tomography
• 4-dimensional positron emission tomography/computed tomography

KEY POINTS

- Fast helical computed tomography (CT) does not reduce misregistration between the CT and the positron emission tomography (PET) data.
- Average CT matches PET in temporal resolution and improves registration with the PET data.
- Radiation dose of average CT can be as low as less than 1 mSv.
- 4-dimensional CT has been successfully adopted in radiation therapy treatment planning.
- List-mode data acquisition improves the work flow of 4-dimensional PET.
- More promising approaches are being explored in clinical and research settings.

INTRODUCTION

Although the idea of positron emission tomography/computed tomography (PET/CT) emerged in 1993, with the first prototype designed in 1998,[1] it was not until 2001 when the first commercial PET/CT scanner became available.[2] Before the introduction of PET/CT technology, the CT and the PET data were acquired in 2 different scanners. Fusion of the PET and CT data was performed using software techniques.[3,4] Registration of the PET and CT data was relatively accurate for brain studies using rigid transformation but not very successful for the other regions of the body, in particular in the thorax and the abdomen, due to the difficulty of repositioning the patient in 2 separate sessions and the nonrigid nature of the organs.

This work was supported by the Swiss National Science Foundation under grant SNSF 31003A-135576, Geneva Cancer League and the Indo-Swiss Joint Research Programme ISJRP 138866.
Conflict of Interest Notification: Dr Tinsu Pan is the owner of Texas Medical Imaging Consultants, LLC.
[a] Department of Imaging Physics, MD Anderson Cancer Center, The University of Texas, Unit 1352, 1515 Holcome Boulevard, Houston, TX 77030, USA; [b] Division of Nuclear Medicine and Molecular Imaging, Geneva University Hospital, CH-1211 Geneva, Switzerland; [c] Geneva Neuroscience Center, Geneva University, CH-1211 Geneva, Switzerland; [d] Department of Nuclear Medicine and Molecular Imaging, University Medical Center Groningen, University of Groningen, 9700 RB Groningen, Netherlands
* Corresponding author.
E-mail address: tpan@mdanderson.org

PET Clin 8 (2013) 37–50
http://dx.doi.org/10.1016/j.cpet.2012.09.009

The advent of PET/CT scanners has made possible for the first time that a single imaging table transporting the patient between PET and CT to hardware fuse the PET and CT data sets. It has been shown that hardware fusion is more accurate than software fusion in clinical diagnosis, staging and restaging of many cancer types such as tumor infiltration of adjacent structures that could not be conclusively assessed using the separate CT and PET data.[5–7] There are over 3000 PET/CT scanners installed worldwide,[8,9] and stand-alone PET scanners have not been in production since 2005.[10] Fluorodeoxyglucose (^{18}F-FDG) is the major pharmaceutical agent in PET/CT, and it has been approved in the United States for diagnosis, staging, and restaging of lung cancer, colorectal cancer, esophageal cancer, head and neck cancer, lymphoma, and melanoma since 1998.[11] In addition, PET/CT has been approved for staging and restaging and for therapeutic monitoring of breast cancer.

The application of PET/CT is mainly in oncology with ^{18}F-FDG[12–16] and in cardiology with ^{82}Rb or ^{13}N-NH_3 for myocardial perfusion imaging.[17] PET/CT also plays an important role in biologically guided radiation therapy[18,19] and treatment response assessment.[20,21] Integration of functional PET data with anatomic CT data should be a standard in radiation therapy.[14,22] However, it remains a challenge to quantify the improvement of simulation with PET/CT over CT in radiation treatment planning, as conclusive clinical data are not yet available. Early studies have found PET/CT has advantages over CT in standardization of volume delineation,[23,24] in reduction of the risk for geometric misses,[25] and in minimization of radiation dose to the nontarget organs.[13,15,26] Use of PET/CT is expected to grow as more molecular targeted imaging agents are being developed.[27,28]

There are challenges in PET/CT imaging. PET needs CT data for tumor localization, attenuation correction, and quantification. The use of CT-based attenuation correction (CT-AC) for PET data has greatly improved the throughput of PET/CT scan and patient comfort when a CT scan of 100 cm can be performed in less than 20 seconds on a 16-slice PET/CT and less than 10 seconds on a 64-slice PET/CT. In general, 16-slice CT is sufficient for tumor imaging, and 64-slice CT is required for coronary artery imaging. The progress in CT-AC methodology has been immense in the last few years, the main opportunities arising from the development of both optimized scanning protocols and innovative image processing algorithms. However, the use of CT images for attenuation correction of PET data is known to produce artifacts in the resulting PET images in some cases.[29,30] This includes artifacts resulting from the polychromaticity of x-ray photons and resulting beam hardening, misregistration between emission and transmission data, the use of contrast-enhanced CT, truncation resulting from the limited field-of-view of CT, the presence of metallic objects, and artifacts arising from x-ray scatter in CT images.[31]

Application of PET/CT in nuclear medicine or radiology is a detection and quantitation task based on standardized uptake value (SUV).[32–34] Physicians can sometimes mentally construct an ideal image even if the images are with artifacts. If the artifacts are not significant, they can simply be read through. Any mismatch between the CT and the PET data in PET/CT may compromise localization and quantification of the PET data. For example, administration of the intravenous contrast in the CT scan before the PET scan may cause artifacts in the attenuation-corrected PET data. The high-attenuation contrast media can cause overcorrection of the PET data. This artifact can appear focal and mimic a malignant lymph node in the axilla or supraclavicular area.[35] Patient motion between the CT and the PET scan is another source of artifacts. Registration with the rigid translation and/or rotation of the CT images to match with the PET data may be sufficient to fix the brain images such as those shown in **Fig. 1**. This article will focus on attenuation correction strategies in PET/CT to mitigate the respiration-induced artifacts in PET/CT and 4-dimensional PET/CT, which are more difficult to correct with postprocessing registration software.

CAUSES OF MISREGISTRATION DUE TO RESPIRATORY MOTION

Misregistration between the CT and PET images due to respiratory motion in the thorax and abdomen was reported soon after the first commercial PET/CT was introduced in 2001[36–39] and has been among the most researched topics in PET/CT. It has impact on radiation therapy, which relies on accurate localization of the tumor for targeted treatment. Radiation oncologists cannot reliably plan therapy by assuming the target tumor at a certain location when it is not the case. They may not be familiar with pitfalls associated with PET/CT imaging, and as such, they generally rely on PET/CT images and the diagnosis and staging information provided by nuclear medicine physicians or radiologists to treat their patients. Both the location and extent of tumor are critical to the success of the process.

Myocardial perfusion imaging with PET/CT also relies on accurate quantification of the PET data,

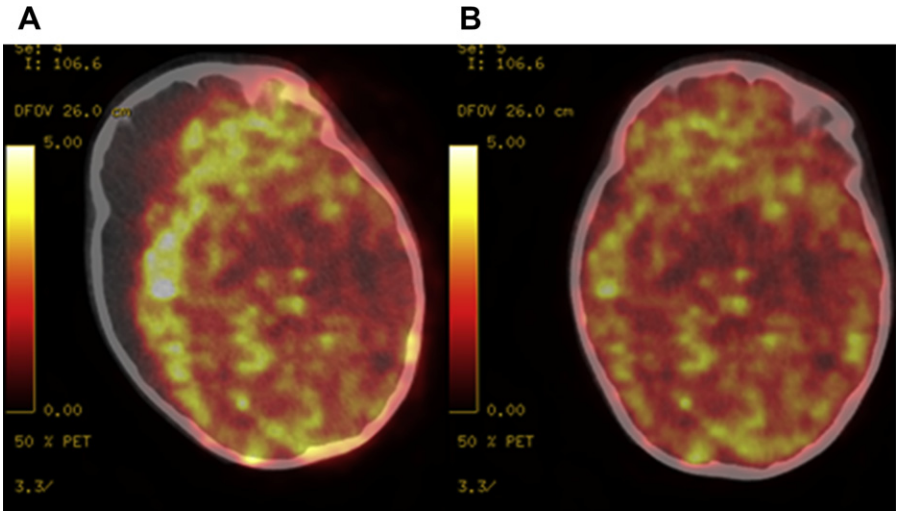

Fig. 1. (*A*) An example of overcorrection and undercorrection of the PET data due to misregistration of the CT and the PET data from the patient motion is shown. (*B*) After applying registration to align the CT and the PET data, improvement in quantification based on the registered PET and CT data is shown.

which depends on accurate registration of CT and PET images for attenuation correction. In general, accurate quantification of the PET images is more critical for myocardial perfusion imaging in cardiology and treatment planning in radiation therapy than for nuclear medicine because of the targeted imaging nature of cardiology and radiation therapy versus whole-body PET imaging in nuclear medicine.

A fast CT scan can cover 100 cm in 10 to 20 seconds, and fast CT gantry rotation can freeze the breathing state in each CT slice. On the other hand, PET takes 2 to 5 minutes to acquire the data of every 15 to 21 cm in the cranial–caudal direction.[40,41] The temporal resolutions of CT and PET are very different: less than 1 second for CT and about 1 respiratory cycle for PET from averaging the PET data of many respiratory cycles. **Fig. 2** shows an example of 2 CT images at the same slice location of 2 different breathing conditions: free-breathing and deep-inspiration breath-hold. Different breathing states in CT slices and mismatch of the temporal resolution between CT and PET can cause a misalignment of the tumor or the heart position between the CT and the PET data, and compromise quantification of the PET data.[42]

The current design of PET/CT only matches the spatial resolution of the CT and PET data by blurring the CT images so that the spatial resolution of the CT images matches with the spatial resolution of the PET images. There has been no attempt from the manufacturers to match the temporal resolutions of CT and PET for a routine whole-body PET/CT scan. One limitation in PET/CT imaging is that the acquisition time cannot be too long. It is because the patient's arms are normally raised up over the head during data acquisition. In this position, an average person can maintain a still position for about 15 to 30 minutes at maximum.

Fig. 2. CT images of the same patient at the same slice location for (*A*) free breathing, (*B*) deep-inspiration breath hold and (*C*) superposition of the 2 CT images in (*A*) and (*B*) to illustrate a potential difference in anatomy between 2 different breathing states.

Mismatch between the CT and the PET data can be identified by a curvilinear white band or photon-penic region near the diaphragm in the PET images (**Fig. 3**). Existence of the white band only suggests a misregistration near the diaphragm and does not mean misregistration at the tumor location. It is possible to have good registration at the tumor location but poor registration at the diaphragm position or vice versa. Note that the heart is always on top of the diaphragm; the problem of misregistration in cardiac PET can be identified more easily in this situation.

Since people spend more time in expiration than in inspiration, the PET data averaged over several minutes are closer to the end-expiration than the end-inspiration. If the CT data are acquired near the end-expiration, then the CT and the PET data may register together better. On the other hand, if the CT data are acquired in or near the end-inspiration, the inflated lungs of inspiration will be larger than the deflated lungs of expiration. The larger area of the inflated lungs in CT renders less attenuation correction in the reconstruction of the PET data near the diaphragm where the inflated lungs push the diaphragm lower in CT than the average diaphragm position in PET. The result is a white band region identified as the misregistered region or the photon-penic region.

FREQUENCY OF MISREGISTRATION

The rate of misregistration can be as high as 68%[43] to 84%.[37] However, it only impacted 2% of diagnosis in the whole-body PET/CT with ^{18}F-FDG[44] but caused false-positive results in 40% of the cardiac PET/CT studies with ^{82}Rb.[45] In whole-body PET/CT, many lesions may not be close to the diaphragm, where most misregistrations occur; and as such, the task of diagnosis may not be compromised by a misregistration between the CT and the PET data. Since the heart is right above the diaphragm, and diagnosis of a cardiac PET is dependent on accurate quantification of the PET data, a more stringent requirement in registration is needed for the cardiac PET/CT than for whole-body PET/CT. For radiation therapy, there has been a study of 216 patients in quantification and gross tumor volume (GTV) delineation.[43] In this study, 68% had respiratory artifacts, and 10% of the misregistrations could cause an SUV change of over 25%, a threshold indicating a response to therapy.[46] Tumors less than 50 cm^3 near the diaphragm could have a change of the centroid tumor location of 2.4 mm, a GTV change of 154% and an SUV change of 21%.

FAST CT DOES NOT REDUCE MISREGISTRATION

It is important to recognize that fast translation of the CT table during a helical CT scan may not eliminate or reduce misregistration between the CT and the PET data. It was suggested that CT images register better between slices if the CT scanner has at least 6 slices.[41] It is true that fast CT gantry rotation helps reduce motion artifacts in each CT slice. However, better registration between slices

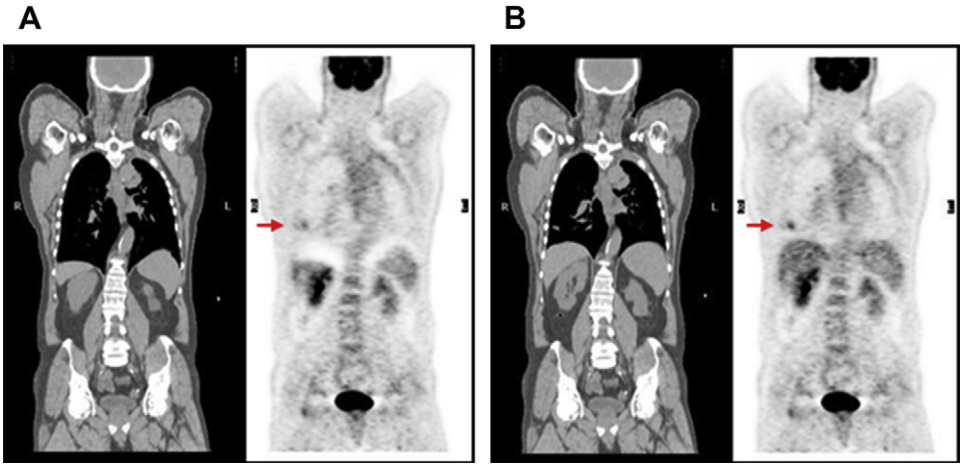

Fig. 3. (*A*) When the CT data have a lower diaphragm position than the PET data, a photo-panic region with an underestimation of FDG uptake in SUV = 2.3 around the diaphragm is shown. *(B)* After correction of the PET data with the average CT data, the photo-penic region disappeared and the SUV of the tumor (pointed by the arrow) increased by 57% from 2.3 to 3.6. (*Reproduced from* Zaidi H, Pan T. Recent advances in hybrid imaging for radiation therapy planning: the cutting edge. PET Clinics 2011;6(2):216; with permission.)

in CT and less motion artifacts in each CT slice do not translate into better registration between the CT and the PET data. Coaching the patient to hold breath at midexpiration during CT acquisition has been suggested.[47] The outcomes were mixed, because coaching patient to hold breath at a certain state during CT data acquisition is not reliable both from the patient and the technologist operating the PET/CT scanner perspectives. In a study of 100 patients coached to hold breath at midexpiration, 50 patient data sets exhibited a misalignment (>1 cm) between the CT and the PET data.[42]

It is clear that as long as the CT scan is conducted when the patient is free breathing, there is always possibility that the CT and the PET data may be misaligned, because some CT slices are taken at inspiration, and some at expiration while the PET data are averaged over several minutes. The distance between 2 end-expiration phases can become longer (or shorter) with a faster (or slower) speed helical CT scan. **Fig. 4** shows an example of CT images taken when the patient was free breathing during a CT scan at the speed of 1.72 cm/s. There were respiratory artifacts on the abdomen and cardiac pulsation artifacts on the heart. These artifacts were not discernible in the review of each individual CT slice. By measuring the distance between the adjacent peaks of the respiratory (cardiac pulsation) artifacts and dividing the distance to the table translation speed of the helical CT scan, one can estimate the breathing cycle (the heart rate) of the patient. These artifacts were due to the respiration and the heart beat of the patient. Presentation of the artifacts depends on the speed of the helical CT scan and the breathing patterns of the patient during the fast CT scan.

Fig. 4. Example of a CT image taken when the patient was free breathing during a CT scan at the speed of 1.72 cm/s. There were respiratory artifacts (pointed by three arrows) on the abdomen and cardiac pulsation artifacts (pointed by an arrow to the heart) on the heart. These artifacts were not obvious in each CT slice. Presentation of the artifacts depends on the speed of the helical CT scan and the breathing patterns of the patient during the CT scan. (*Reproduced from* Zaidi H, Pan T. Recent advances in hybrid imaging for radiation therapy planning: the cutting edge. PET Clinics 2011;6(2):212; with permission.)

AVERAGE CT OF LESS THAN 1 mSv REDUCES MISREGISTRATION

Many potential solutions have been suggested to accommodate differences between breathing patterns including retrospective AC using free breathing CT,[48] the use of optimal CT acquisition protocols,[49,50] respiratory averaged CT,[42,51–53,59] interpolated average CT,[54,55] phased CT acquisitions,[56–58] cine CT acquisition,[59] respiratory correlated acquisitions,[60–62] deep-inspiration breath-hold acquisition,[44,63–65] and the use of respiratory-gated PET/CT acquisitions.[66–75]

One approach to improve registration between the CT and the PET data is to bring the temporal resolution of the CT images to that of the PET data.[42] Recognizing the fact that PET is averaged over many breath cycles, a CT image averaged over 1 breath cycle should improve registration between the CT and the PET data. **Fig. 3** shows an example of misregistration between the CT and the PET data, and correction of misregistration with average CT to improve tumor quantification. This concept has also been shown to be effective in attenuation correction of the PET data in cardiac imaging.[51]

Acquiring average CT can be accomplished by scanning at the same slice location over a breath cycle at a high-speed gantry rotation to achieve temporal resolution of less than 1 second for each acquired CT image. The CT images of many phases in a respiratory cycle, mostly free of motion artifacts, are averaged for average CT (**Fig. 5**). The conventional approach using the slow-scan CT of 4 second gantry rotation to generate average CT is ineffective and should be discouraged.[51,76] **Fig. 6** shows a clinical example of the same patient scanned with the slow-scan CT of 4 seconds per gantry rotation and average CT of fast gantry rotation of 0.5 seconds for 4 seconds. The image generated by a slow 4-second gantry had motion artifacts, because the projection data of a slow 4-second CT were inconsistent over 1 revolution of the CT scan. In the approach of using fast gantry rotation for average CT, each CT image was

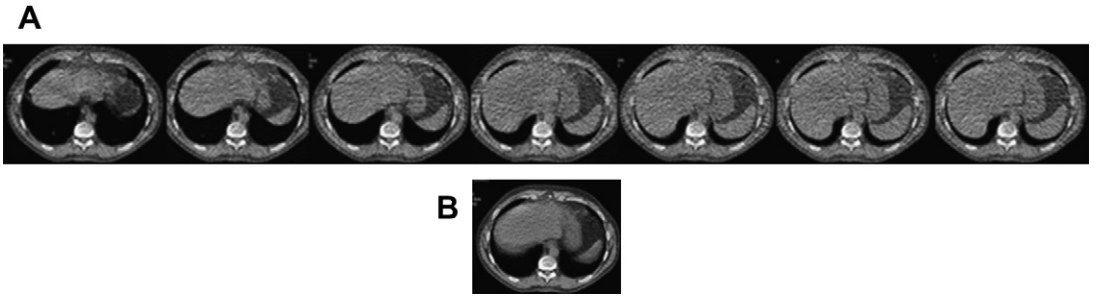

Fig. 5. Averaging of the CT images taken at the same slice location over a respiratory cycle in (*A*) generates the average CT image in (*B*). Each CT image in (*A*) was taken at 5 mAs (10 mA and 0.5 second gantry rotation) on the GE Light Speed CT scanner (GE Healthcare, Waukesha, WI).

acquired over a sub-second CT gantry rotation and was without motion artifacts. Averaging over a breath cycle of these high temporal resolution CT images can produce an average CT image with a similar temporal resolution as the PET data.

Cine CT and low-pitch helical CT (pitch <0.1) scans can be adopted to obtain average CT, and both have been used in 4-dimensional CT imaging.[77–79] However, it is not clear whether the setup of 4-dimensional CT imaging primarily for the assessment of tumor motion is ideal for obtaining average CT when most PET/CT scanners are in nuclear medicine and are without the respiratory monitoring device needed for 4-dimensional CT. A practical approach is to acquire average CT without a respiratory monitoring device to improve quantification of the PET data.[51,80] The additional radiation dose for average CT can be less than 1 mSv, and the additional scan time is less than one minute and will not impact the overall scan time of a PET/CT procedure. Selection of optimum parameters for acquiring average CT with cine CT or low-pitch helical CT has been reported.[52]

In terms of temporal resolution, average CT is about 1 respiratory cycle, while the transmission map acquired with rotating rod sources of ^{68}Ge and ^{137}Cs is also about 1 respiratory cycle from averaging of many respiratory cycles. Average CT can be used to approximate the transmission map in terms of temporal resolution. Pan and colleagues[42] demonstrated that registration of the CT and PET data can be improved with average CT in tumor imaging and myocardial perfusion imaging.[51] Papathanassiou and colleagues[81] and Osman and colleagues[37] showed that using the attenuation map from transmission rod sources to correct for the PET images would not produce the curvilinear cold artifacts in the PET data of PET/CT. Transmission rod source is only available in the first-generation PET/CT scanners and not available on the newer PET/CT scanners. The advantages of average CT over transmission rod sources are short acquisition time (1 minutes for CT, and 10 min/15 cm in transmission) and high photon flux and less noisy attenuation maps. The disadvantages are higher radiation dose of less than 1 mSv from average CT than about 0.13 mSv from the transmission rod sources.[82] Radiation therapy has embraced the use of average CT for dose calculation.[83] Since most of

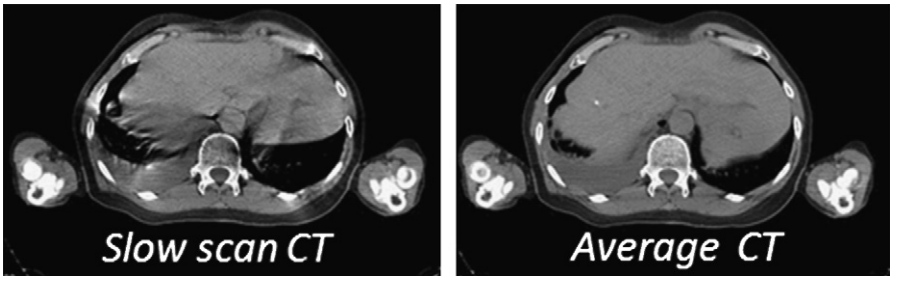

Fig. 6. Comparison of slow-scan CT and average CT of the same patient. The slow-scan CT was taken on a single gantry rotation of 4 seconds, and the average CT was taken from the average of 8 images of 0.5 second gantry rotation for 4 seconds. The artifacts in the slow-scan CT due to reconstruction of the inconsistent CT data in the 4-second scan due to respiration are not in the average CT image. (*Reproduced from* Pan T, Mawlawi O, Luo D, et al. Attenuation correction of PET cardiac data with low-dose average CT in PET/CT. Med Phys 2006;33(10):3937; with permission.)

the new PET/CT scanners are not equipped with transmission rod sources, average CT can serve as an alternative for transmission rod sources. **Fig. 7** shows an example of combining the fast helical CT images and the average CT images of the target tumor area to minimize the area of radiation incurred by the average CT scan. In a whole-body PET/CT examination, the CT images are typically acquired before PET. The technologist can determine if an additional average CT scan is needed when the CT and the PET images of the thorax and the abdomen are available before completion of the PET scan. **Fig. 8** shows an example of average CT improving the registration and quantification of a lymph node. **Fig. 9** shows an example of improvement in the registration and quantification of a lung tumor near the diaphragm and the heart.

Fig. 10 shows an example of misregistration that caused a false-negative diagnosis and a change of the gross target volume for radiation therapy. In the era of image-guided radiation therapy to deliver a very high dose at a great precision, it is very important to pay attention to any misregistration between the CT and the PET images during tumor delineation.

4-DIMENSIONAL PET IMAGING

4-dimensional PET was first developed for cardiac imaging to assess myocardial motion and to obtain ejection fraction 3 decades ago.[84] It was adopted for tumor imaging of the thorax almost a decade ago,[60,66–68] about the same time when 4-dimensional CT was launched.[62,77–79,85] Today, 4-dimensional CT has been accepted as a standard practice in CT imaging of tumor motion for radiation therapy. 4-dimensional PET is still not yet widely accepted as a standard practice. It may be that PET is primarily used for clinical diagnosis and staging, and that a 4-dimensional PET scan is typically conducted after a whole-body PET scan. The total scan time may become too long for any patient to stay still for the 4-dimensional PET imaging.

In 4-dimensional PET, the data are split into several exclusive bins. For example, there can be 8 bins of 500 milliseconds for an average respiratory cycle of 4 seconds. Because of insufficient statistics of photons obtained in PET imaging of 2 to 5 minutes for the selection of 8 bins in each bed location, the duration of a 4-dimensional PET scan has to be over 5 minutes to compensate for the fewer photons recorded in each bin. It may be necessary to scan 2 bed positions if a tumor or the heart is not at the center of the PET detector field of view to compensate for the high sensitivity at the center and the low sensitivity at the edge of the PET detector in 3-dimensional data acquisition without septa.

Image reconstruction of 4-dimensional PET is performed on the data of each bin, and the result is a set of 3-dimensional PET images over a respiratory cycle for assessment of tumor motion and quantification. Even though the number of photons in each bin can be small, resulting in higher noise in

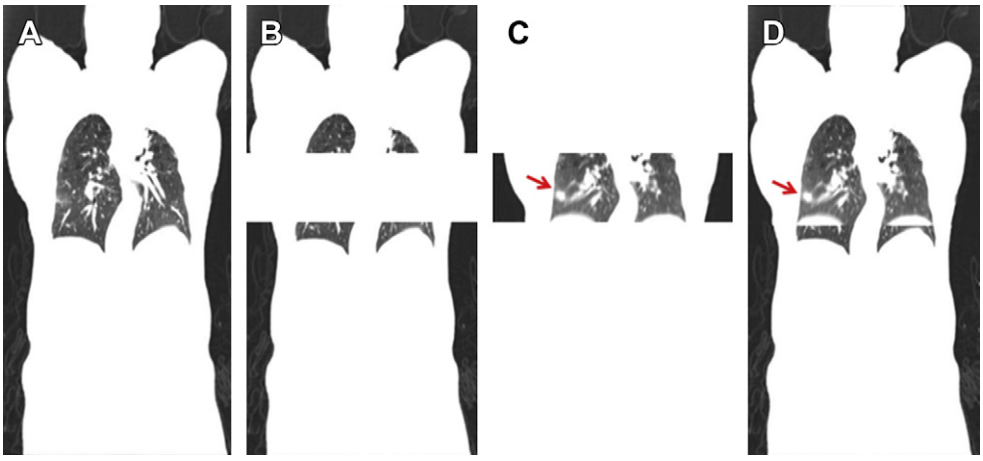

Fig. 7. (*A*) Conventional CT acquired in free breathing; (*B*) the CT images in (*A*) not containing the region containing the tumor; (*C*) the CT images containing the tumor (*pointed by an arrow*) obtained with average CT; and (*D*) combination of (*B*) and (*C*) to make an image for attenuation correction of the PET data. (*Reproduced from* Pan T, Mawlawi O, Nehmeh SA, et al. Attenuation correction of PET images with respiration-averaged CT images in PET/CT. J Nucl Med 2005;46(9):1483; with permission.)

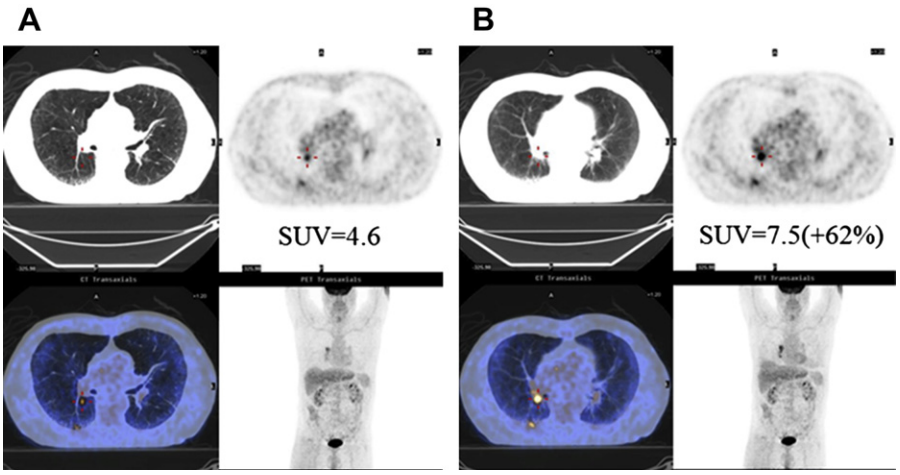

Fig. 8. (*A*) The lymph node shown in PET did not register with the CT and had an SUV of 4.6. (*B*) After attenuation correction with average CT, which registered better with the PET data, the lymph node had an SUV value of 7.5, a 62% increase in SUV. (*Reproduced from* Pan T, Mawlawi O, Nehmeh SA, et al. Attenuation correction of PET images with respiration-averaged CT images in PET/CT. J Nucl Med 2005;46(9):1485; with permission.)

the 4-dimensional PET images,[86] the 4D PET images can potentially be used for accurate assessment of FDG uptake.[68]

Most modern PET/CT scanners are equipped with the list-mode data acquisition, whereby events from each coincidence pair of 511 keV photons can be stored in a list stream for subsequent static, dynamic, or gated reconstruction (**Fig. 11**). List-mode data acquisition can be performed with either cardiac or respiratory triggering during a normal static image acquisition.[87] This functionality offers the capability of retrospectively mapping the coincidence events into multiple phases/bins for the reconstruction of 4-dimensional PET images. PET scanners can be configured to acquire the list-mode data, which can produce prospectively static PET data as a standard data set and retrospectively 4-dimensional PET data to freeze the tumor motion. It is still cumbersome to acquire 4-dimensional PET data due to its prolonged acquisition time. However, it is expected that with the introduction of advanced detector technologies, large detector coverage for higher sensitivity, and incorporation of time-of-flight information in

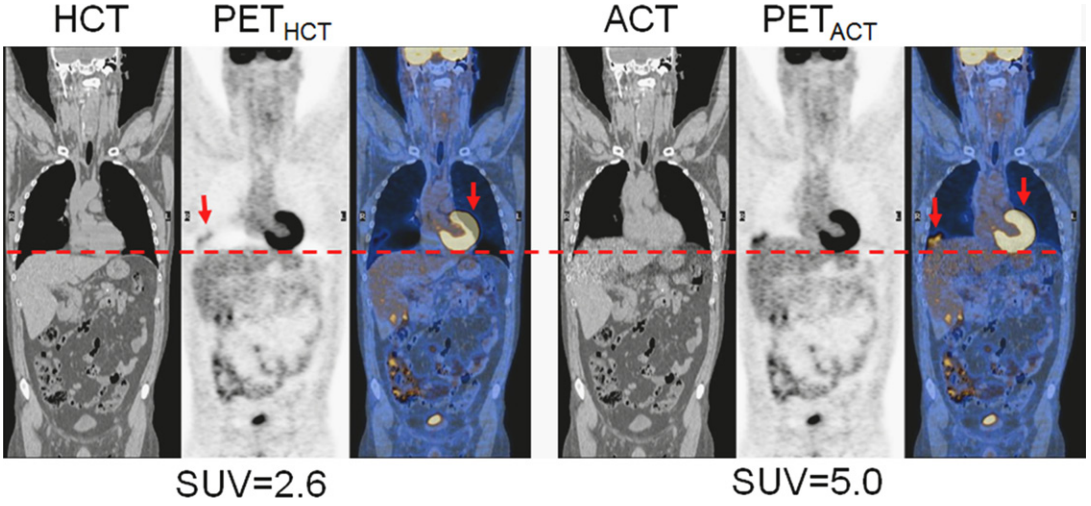

Fig. 9. The standard set of the helical CT (HCT) and the PET data corrected with the HCT is shown in the left panel. Misregistration of the tumor and the heart can be identified and pointed by arrows. Attenuation correction with the average CT (ACT) data is in the right panel. The SUV of the tumor (pointed by an arrow) increased from 2.6 to 5.0. The activity in the heart region (pointed by an arrow) also increased due to the improved registration of the PET and ACT data.

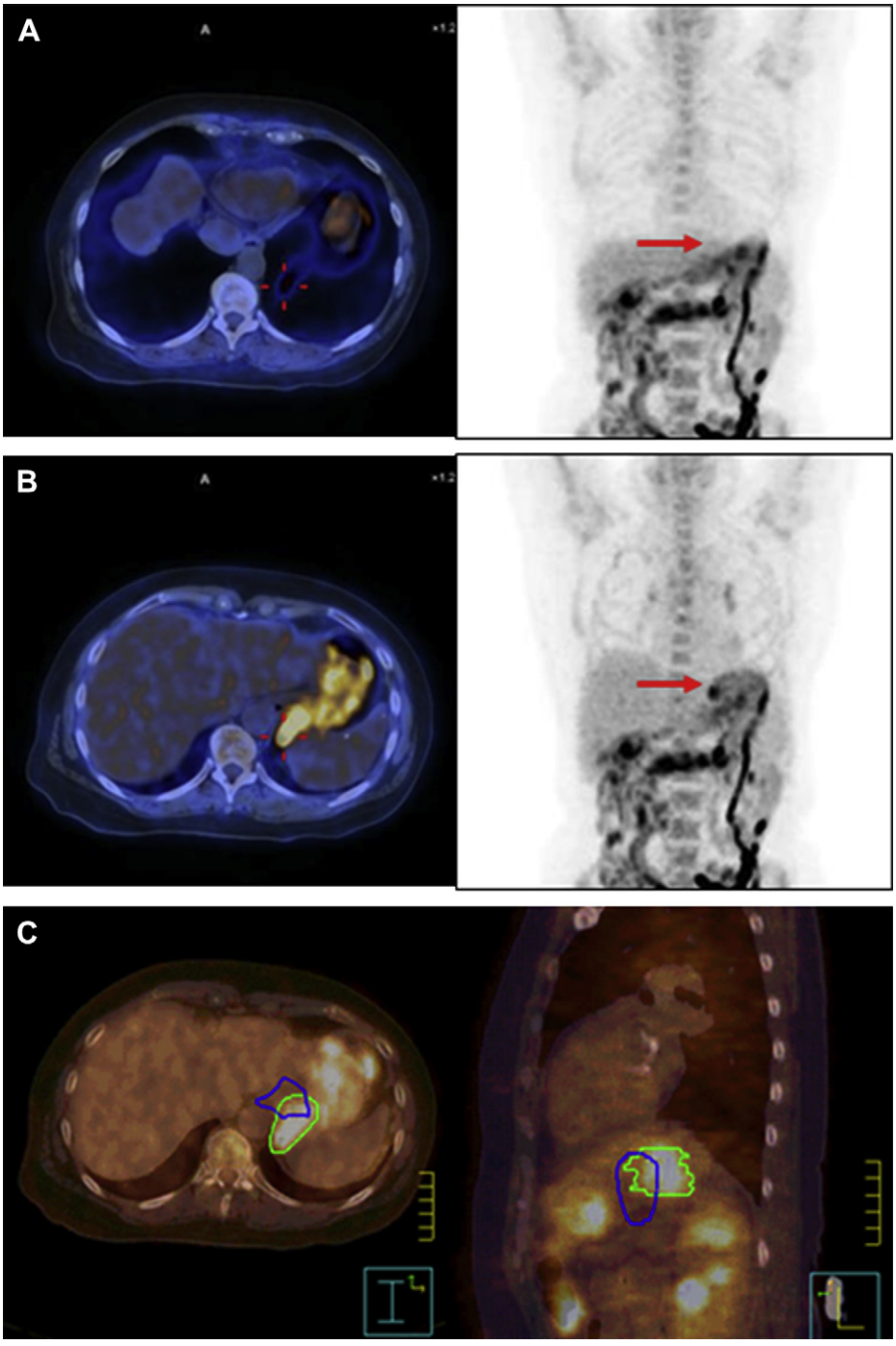

Fig. 10. PET/CT images of a 69 year-old woman with an esophageal tumor after induction chemotherapy. (*A*) An axial slice of the fused clinical CT and PET image at the level of the esophageal tumor (*left*) and the PET image in coronal view (*right*). The diagnosis indicated that the patient had a positive response to the chemotherapy. After removal of the misalignment by average CT, the tumor reappeared in the same PET data set in (*B*). The arrows point to the tumor location. The gross target volumes drawn in the images of (*A*) and (*B*) are shown in blue and in green, respectively, in (C). The patient was treated with the tumor volume in green, and the diagnostic report was corrected by the average CT. (*Reproduced from* Pan T, Mawlawi O. PET/CT in radiation oncology. Med Phys 2008;35(11):4960; with permission.)

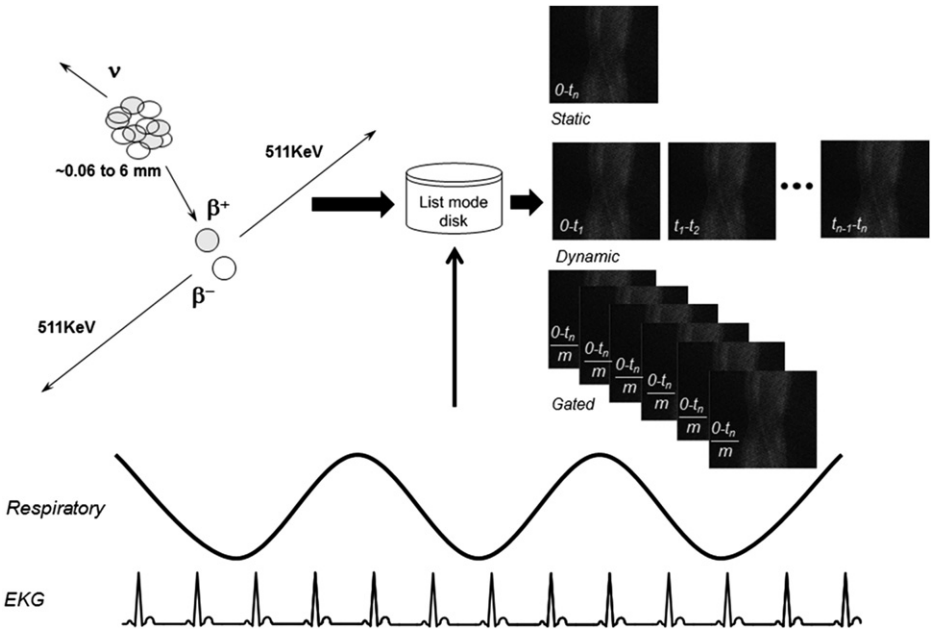

Fig. 11. Schematic diagram of the list-mode data acquisition. The positron coming out of positron emitters such as ^{18}F or ^{82}Rb travels a distance of average 0.06 mm for ^{18}F or 6 mm for ^{82}Rb. The larger the positron energy, the longer the distance it travels. An annihilation event occurs when a positron meets with an electron to emit two 511 keV energy photons and is detected by a pair of PET detectors. List-mode acquisition records the events and the physiologic signal such as the electrocardiogram and/or respiratory signal to guide image reconstruction. Out of the list-mode data acquisition, one can reconstruct the static images of time 0 to t_n, or dynamic images of time 0 to t_1, t_1 to t_2, …, t_{n-1} to t_n or *m* gated images of time 0 to t_n. Each picture represents a sinogram for reconstruction.

3-dimensional image reconstruction to better cope with the increased noise from randoms and scatter in 3-dimensional data acquisition. The limitation in acquisition time will be lifted, 4-dimensional PET will become a clinically feasible solution to improve the quantification accuracy of a tumor or the heart in motion.

4-DIMENSIONAL PET/CT IMAGING

4-dimensional CT[77–79] may be needed for accurate quantification of 4-dimensional PET data, as each phase of PET data may need its own CT data for attenuation correction.[68] Four-dimensional CT has found its acceptance in radiation therapy for providing the gated CT images of multiple phases over a respiratory cycle to assist contouring the extent of tumor motion. Four-dimensional CT takes less time in data acquisition than 4-dimensional PET does. It normally takes less than 2 minutes to cover 35 cm in the superior–inferior direction on an 8- or 16-slice CT. The scan coverage of 4-dimensional CT for radiation therapy is typically the whole lung, while the coverage for average CT should be limited for the tumor or the heart region for diagnosis. Radiation dose for 4-dimensional CT is about 50 mGy, and should be less than 5 mGy for average CT. Two data acquisition modes can be used in 4-dimensional CT: cine CT and low-pitch helical

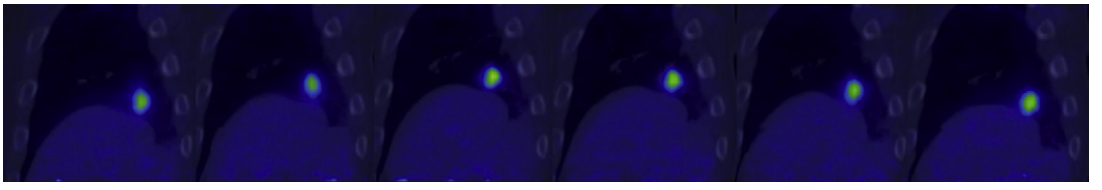

Fig. 12. A 4-dimensional PET/CT patient study. The acquisition time for the 4-dimensional PET scan was 13 minutes, and the PET data were gated into 6 phases. Attenuation of the 4-dimensional PET data was corrected with the corresponding 4-dimensional CT data. Quantification of the tumor in SUV went from 5.0 in the static PET scan without gating to 8.5 in the end-expiration phase of the 4-dimensional PET scan.

CT. Both acquisitions scan the prescribed volume for over 1 breath cycle plus 1 (or 2/3) gantry rotation cycle. Cine CT uses less radiation and generates thinner slices than low-pitch helical CT. Low-pitch helical CT scans are slightly faster than cine CT, because they do not pause between 2 table positions as in cine CT.[88] The cine CT based 4-dimensional CT is available on 4-, 8-, 16-, and 64-slice CT scanners, whereas the low-pitch helical CT-based 4-dimensional CT is only available on newer 16- and 64-slice CT scanners. Four-dimensional CT is a part of 4-dimensional PET/CT if phase-to-phase matching of the attenuation map is desired in 4-dimensional PET imaging.[56,61,68,69] **Fig. 12** illustrates an example of 4-dimensional PET/CT scan of 6 phases over 13 minutes of data acquisition. Quantification of the tumor in SUV changed from 5 in the static PET image without gating to 8.5 at the end-expiration phase in this example. Model-based image reconstruction can also be applied to 4-dimensional PET,[86] based on the tumor motion from 4-dimensional CT, to deform/register the multiple phases of PET data to a single motion freeze PET data set to reduce the noise in 4-dimensional PET data and to improve PET quantification.[89]

SUMMARY

There has been a tremendous effort in improving both PET/CT and 4-dimensional PET/CT imaging in the last decade. With the development of 4-dimensional CT, the difficulties in imaging the tumor motion with CT in the thorax or the abdomen have been largely eliminated. List-mode data acquisition, although not a new concept, has been very useful in making the workflow of postprocessing the 4-dimensional PET data easier than before. Average CT derived from averaging the high temporal resolution CT images acquired over a respiratory cycle has been shown to be effective in improving the registration of the CT and the PET data, resulting in improvement on quantification of the PET data both for tumor imaging and cardiac imaging. Radiation dose of average CT can be reduced to less than 1 mSv, and application of average CT can be limited to only patients whose PET data and CT data do not register. Four-dimensional PET and 4-dimensional PET/CT are emerging as the next frontier for researchers and clinicians to put into clinical use. The bottleneck in 4-dimensional PET and 4-dimensional PET/CT is the long acquisition time for acquiring the 4-dimensional PET data. It is hoped that future instrumentation can improve the sensitivity of PET imaging so that every whole-body PET scan can become a 4-dimensional PET scan without any significant increase of the scan time.

REFERENCES

1. Beyer T, Townsend DW, Brun T, et al. A combined PET/CT scanner for clinical oncology. J Nucl Med 2000;41(8):1369–79.
2. Townsend DW, Beyer T. A combined PET/CT scanner: the path to true image fusion. Br J Radiol 2002;75:S24–30.
3. Hutton BF, Braun M. Software for image registration: algorithms, accuracy, efficacy. Semin Nucl Med 2003;33(3):180–92.
4. Slomka P, Baum R. Multimodality image registration with software: state-of-the-art. Eur J Nucl Med Mol Imaging 2009;36(Suppl 1):44–55.
5. Reinartz P, Wieres FJ, Schneider W, et al. Side-by-side reading of PET and CT scans in oncology: which patients might profit from integrated PET/CT? Eur J Nucl Med Mol Imaging 2004;31(11):1456–61.
6. Wahl RL. Why nearly all PET of abdominal and pelvic cancers will be performed as PET/CT. J Nucl Med 2004;45:82S–95S.
7. Goerres GW, von Schulthess GK, Steinert HC. Why most PET of lung and head-and-neck cancer will be PET/CT. J Nucl Med 2004;45(Suppl 1):66S–71S.
8. Mawlawi O, Townsend DW. Multimodality imaging: an update on PET/CT technology. Eur J Nucl Med Mol Imagin 2009;36(Suppl 1):S15–29.
9. Hricak H, Choi BI, Scott AM, et al. Global trends in hybrid imaging. Radiology 2010;257(2):498–506.
10. Blodgett TM, Meltzer CC, Townsend DW. PET/CT: form and function. Radiology 2007;242(2):360–85.
11. Rohren EM, Turkington TG, Coleman RE. Clinical applications of PET in oncology. Radiology 2004;231(2):305–32.
12. Bradley J, Thorstad WL, Mutic S, et al. Impact of FDG-PET on radiation therapy volume delineation in non-small-cell lung cancer. Int J Radiat Oncol Biol Phys 2004;59(1):78–86.
13. Ciernik IF, Dizendorf E, Baumert BG, et al. Radiation treatment planning with an integrated positron emission and computer tomography (PET/CT): a feasibility study. Int J Radiat Oncol Biol Phys 2003;57(3):853–63.
14. Mah K, Caldwell CB, Ung YC, et al. The impact of (18)FDG-PET on target and critical organs in CT-based treatment planning of patients with poorly defined non-small-cell lung carcinoma: a prospective study. Int J Radiat Oncol Biol Phys 2002;52(2):339–50.
15. van Baardwijk A, Baumert BG, Bosmans G, et al. The current status of FDG-PET in tumour volume definition in radiotherapy treatment planning. Cancer Treat Rev 2006;32(4):245–60.

16. Messa C, Di Muzio N, Picchio M, et al. PET/CT and radiotherapy. Q J Nucl Med Mol Imaging 2006;50(1): 4–14.
17. Di Carli MF, Dorbala S, Meserve J, et al. Clinical myocardial perfusion PET/CT. J Nucl Med 2007; 48(5):783–93.
18. Stewart RD, Li XA. BGRT: biologically guided radiation therapy - the future is fast approaching. Med Phys 2007;34(10):3739–51.
19. Zaidi H, Pan T. Recent advances in hybrid imaging for radiation therapy planning: the cutting edge. PET Clinics 2011;6(2):207–26.
20. Weber WA. Monitoring tumor response to therapy with 18F-FLT PET. J Nucl Med 2010;51(6):841–4.
21. Gregory DL, Hicks RJ, Hogg A, et al. Effect of PET/CT on management of patients with non-small cell lung cancer: results of a prospective study with 5-year survival data. J Nucl Med 2012;53(7):1007–15.
22. Zaidi H, Vees H, Wissmeyer M. Molecular PET/CT imaging-guided radiation therapy treatment planning. Acad Radiol 2009;16(9):1108–33.
23. Steenbakkers RJ, Duppen JC, Fitton I, et al. Reduction of observer variation using matched CT-PET for lung cancer delineation: a three-dimensional analysis. Int J Radiat Oncol Biol Phys 2006;64(2): 435–48.
24. Ashamalla H, Rafla S, Parikh K, et al. The contribution of integrated PET/CT to the evolving definition of treatment volumes in radiation treatment planning in lung cancer. Int J Radiat Oncol Biol Phys 2005; 63(4):1016–23.
25. Erdi YE, Rosenzweig K, Erdi AK, et al. Radiotherapy treatment planning for patients with non-small cell lung cancer using positron emission tomography (PET). Radiother Oncol 2002;62(1):51–60.
26. Schwartz DL, Ford EC, Rajendran J, et al. FDG-PET/CT-guided intensity modulated head and neck radiotherapy: a pilot investigation. Head Neck 2005;27(6):478–87.
27. Valliant JF. A bridge not too far: linking disciplines through molecular imaging probes. J Nucl Med 2010;51(8):1258–68.
28. Chao KS, Bosch WR, Mutic S, et al. A novel approach to overcome hypoxic tumor resistance: Cu-ATSM-guided intensity-modulated radiation therapy. Int J Radiat Oncol Biol Phys 2001;49(4): 1171–82.
29. Kinahan PE, Hasegawa BH, Beyer T. X-ray-based attenuation correction for positron emission tomography/computed tomography scanners. Semin Nucl Med 2003;33(3):166–79.
30. Zaidi H, Hasegawa BH. Determination of the attenuation map in emission tomography. J Nucl Med 2003;44(2):291–315.
31. Zaidi H, Montandon ML, Alavi A. Advances in attenuation correction techniques in PET. PET Clinics 2007;2(2):191–217.
32. Zasadny KR, Wahl RL. Standardized uptake values of normal tissues at PET with 2-[fluorine-18]-fluoro-2-deoxy-D-glucose: variations with body weight and a method for correction. Radiology 1993; 189(3):847–50.
33. Keyes JW Jr. SUV: standard uptake or silly useless value? J Nucl Med 1995;36(10):1836–9.
34. Basu S, Zaidi H, Houseni M, et al. Novel quantitative techniques for assessing regional and global function and structure based on modern imaging modalities: implications for normal variation, aging and diseased states. Semin Nucl Med 2007;37(3): 223–39.
35. Antoch G, Freudenberg LS, Egelhof T, et al. Focal tracer uptake: a potential artifact in contrast-enhanced dual-modality PET/CT scans. J Nucl Med 2002;43(10):1339–42.
36. Vogel WV, van Dalen JA, Wiering B, et al. Evaluation of image registration in PET/CT of the liver and recommendations for optimized imaging. J Nucl Med 2007;48(6):910–9.
37. Osman MM, Cohade C, Nakamoto Y, et al. Respiratory motion artifacts on PET emission images obtained using CT attenuation correction on PET-CT. Eur J Nucl Med Mol Imaging 2003;30(4):603–6.
38. Osman MM, Cohade C, Nakamoto Y, et al. Clinically significant inaccurate localization of lesions with PET/CT: frequency in 300 patients. J Nucl Med 2003;44(2):240–3.
39. Goerres GW, Kamel E, Seifert B, et al. Accuracy of image coregistration of pulmonary lesions in patients with non-small cell lung cancer using an integrated PET/CT system. J Nucl Med 2002;43(11):1469–75.
40. Beyer T, Antoch G, Muller S, et al. Acquisition protocol considerations for combined PET/CT imaging. J Nucl Med 2004;45(Suppl 1):25S–35S.
41. Beyer T, Rosenbaum S, Veit P, et al. Respiration artifacts in whole-body (18)F-FDG PET/CT studies with combined PET/CT tomographs employing spiral CT technology with 1 to 16 detector rows. Eur J Nucl Med Mol Imaging 2005;32(12):1429–39.
42. Pan T, Mawlawi O, Nehmeh SA, et al. Attenuation correction of PET images with respiration-averaged CT images in PET/CT. J Nucl Med 2005;46(9):1481–7.
43. Chi PC, Mawlawi O, Luo D, et al. Effects of respiration-averaged computed tomography on positron emission tomography/computed tomography quantification and its potential impact on gross tumor volume delineation. Int J Radiat Oncol Biol Phys 2008;71(3):890–9.
44. Kawano T, Ohtake E, Inoue T. Deep-inspiration breath-hold PET/CT of lung cancer: maximum standardized uptake value analysis of 108 patients. J Nucl Med 2008;49(8):1223–31.
45. Gould KL, Pan T, Loghin C, et al. Frequent diagnostic errors in cardiac PET/CT due to misregistration of CT attenuation and emission PET images: a definitive

analysis of causes, consequences, and corrections. J Nucl Med 2007;48(7):1112–21.
46. Young H, Baum R, Cremerius U, et al. Measurement of clinical and subclinical tumour response using [18F]-fluorodeoxyglucose and positron emission tomography: review and 1999 EORTC recommendations. European Organization for Research and Treatment of Cancer (EORTC) PET Study Group. Eur J Cancer 1999;35(13):1773–82.
47. Goerres GW, Burger C, Schwitter MR, et al. PET/CT of the abdomen: optimizing the patient breathing pattern. Eur Radiol 2003;13(4):734–9.
48. Fitton I, Steenbakkers RJ, Zijp L, et al. Retrospective attenuation correction of PET data for radiotherapy planning using a free breathing CT. Radiother Oncol 2007;83(1):42–8.
49. Gilman MD, Fischman AJ, Krishnasetty V, et al. Optimal CT breathing protocol for combined thoracic PET/CT. AJR Am J Roentgenol 2006;187(5):1357–60.
50. Nye JA, Esteves F, Votaw JR. Minimizing artifacts resulting from respiratory and cardiac motion by optimization of the transmission scan in cardiac PET/CT. Med Phys 2007;34(6):1901–6.
51. Pan T, Mawlawi O, Luo D, et al. Attenuation correction of PET cardiac data with low-dose average CT in PET/CT. Med Phys 2006;33(10):3931–8.
52. Chi PC, Mawlawi O, Nehmeh SA, et al. Design of respiration averaged CT for attenuation correction of the PET data from PET/CT. Med Phys 2007; 34(6):2039–47.
53. Cook RA, Carnes G, Lee TY, et al. Respiration-averaged CT for attenuation correction in canine cardiac PET/CT. J Nucl Med 2007;48(5):811–8.
54. Huang TC, Mok GS, Wang SJ, et al. Attenuation correction of PET images with interpolated average CT for thoracic tumors. Phys Med Biol 2011;56(8): 2559–67.
55. Wu TH, Zhang G, Wang SJ, et al. Low-dose interpolated average CT for attenuation correction in cardiac PET/CT. Nucl Instrum Meth A 2010;619(1–3):361–4.
56. Nagel CC, Bosmans G, Dekker AL, et al. Phased attenuation correction in respiration correlated computed tomography/positron emitted tomography. Med Phys 2006;33(6):1840–7.
57. Wells RG, Ruddy TD, DeKemp RA, et al. Single-phase CT aligned to gated PET for respiratory motion correction in cardiac PET/CT. J Nucl Med 2010;51(8):1182–90.
58. Ponisch F, Richter C, Just U, et al. Attenuation correction of four dimensional (4D) PET using phase-correlated 4D-computed tomography. Phys Med Biol 2008;53(13):N259–68.
59. Alessio AM, Kohlmyer S, Branch K, et al. Cine CT for attenuation correction in cardiac PET/CT. J Nucl Med 2007;48(5):794–801.
60. Nehmeh SA, Erdi YE, Rosenzweig KE, et al. Reduction of respiratory motion artifacts in PET imaging of lung cancer by respiratory correlated dynamic PET: methodology and comparison with respiratory gated PET. J Nucl Med 2003;44(10):1644–8.
61. Erdi YE, Nehmeh SA, Pan T, et al. The CT motion quantitation of lung lesions and its impact on PET-measured SUVs. J Nucl Med 2004;45(8):1287–92.
62. Mageras GS, Pevsner A, Yorke ED, et al. Measurement of lung tumor motion using respiration-correlated CT. Int J Radiat Oncol Biol Phys 2004; 60(3):933–41.
63. Nehmeh SA, Erdi YE, Meirelles GS, et al. Deep-inspiration breath-hold PET/CT of the thorax. J Nucl Med 2007;48(1):22–6.
64. Meirelles GS, Erdi YE, Nehmeh SA, et al. Deep-inspiration breath-hold PET/CT: clinical findings with a new technique for detection and characterization of thoracic lesions. J Nucl Med 2007;48(5):712–9.
65. Torizuka T, Tanizaki Y, Kanno T, et al. Single 20-second acquisition of deep-inspiration breath-hold PET/CT: clinical feasibility for lung cancer. J Nucl Med 2009;50(10):1579–84.
66. Nehmeh SA, Erdi YE, Ling CC, et al. Effect of respiratory gating on reducing lung motion artifacts in PET imaging of lung cancer. Med Phys 2002;29(3): 366–71.
67. Nehmeh SA, Erdi YE, Ling CC, et al. Effect of respiratory gating on quantifying PET images of lung cancer. J Nucl Med 2002;43(7):876–81.
68. Nehmeh SA, Erdi YE, Pan T, et al. Four-dimensional (4D) PET/CT imaging of the thorax. Med Phys 2004; 31(12):3179–86.
69. Nehmeh SA, Erdi YE, Pan T, et al. Quantitation of respiratory motion during 4D-PET/CT acquisition. Med Phys 2004;31(6):1333–8.
70. Boucher L, Rodrigue S, Lecomte R, et al. Respiratory gating for 3-dimensional PET of the thorax: feasibility and initial results. J Nucl Med 2004;45(2):214–9.
71. Pevsner A, Nehmeh SA, Humm JL, et al. Effect of motion on tracer activity determination in CT attenuation corrected PET images: a lung phantom study. Med Phys 2005;32(7):2358–62.
72. Martinez-Möller A, Zikic D, Botnar R, et al. Dual cardiac respiratory gated PET: implementation and results from a feasibility study. Eur J Nucl Med Mol Imaging 2007;34(9):1447–54.
73. Klein GJ, Reutter BW, Ho MH, et al. Real-time system for respiratory-cardiac gating in positron tomography. IEEE Trans Nucl Sci 1998;45(4):2139–43.
74. Visvikis D, Lamare F, Bruyant P, et al. Respiratory motion in positron emission tomography for oncology applications: problems and solutions. Nucl Instr Meth A 2006;569(2):453–7.
75. Rahmim A, Rousset O, Zaidi H. Strategies for motion tracking and correction in PET. PET Clinics 2007; 2(2):251–66.
76. Keall PJ, Mageras GS, Balter JM, et al. The management of respiratory motion in radiation oncology

report of AAPM Task Group 76. Med Phys 2006; 33(10):3874–900.
77. Low DA, Nystrom M, Kalinin E, et al. A method for the reconstruction of four-dimensional synchronized CT scans acquired during free breathing. Med Phys 2003;30(6):1254–63.
78. Pan T, Lee TY, Rietzel E, et al. 4D-CT imaging of a volume influenced by respiratory motion on multi-slice CT. Med Phys 2004;31(2):333–40.
79. Keall PJ, Starkschall G, Shukla H, et al. Acquiring 4D thoracic CT scans using a multislice helical method. Phys Med Biol 2004;49(10):2053–67.
80. Pan T, Sun X, Luo D. Improvement of the cine-CT based 4D-CT imaging. Med Phys 2007;34(11): 4499–503.
81. Papathanassiou D, Becker S, Amir R, et al. Respiratory motion artifact in the liver dome on FDG PET/CT: comparison of attenuation correction with CT and a caesium external source. Eur J Nucl Med Mol Imaging 2005;32(12):1422–8.
82. Wu TH, Huang YH, Lee JJ, et al. Radiation exposure during transmission measurements: comparison between CT- and germanium-based techniques with a current PET scanner. Eur J Nucl Med Mol Imaging 2004;31(1):38–43.
83. Riegel AC, Ahmad M, Sun X, et al. Dose calculation with respiration-averaged CT processed from cine CT without a respiratory surrogate. Med Phys 2008;35(12):5738–47.
84. Hoffman EJ, Phelps ME, Wisenberg G, et al. Electrocardiographic gating in positron emission computed tomography. J Comput Assist Tomogr 1979;3(6): 733–9.
85. Vedam SS, Keall PJ, Kini VR, et al. Acquiring a four-dimensional computed tomography dataset using an external respiratory signal. Phys Med Biol 2003; 48(1):45–62.
86. Rahmim A, Tang J, Zaidi H. Four-dimensional (4D) image reconstruction strategies in dynamic PET: beyond conventional independent frame reconstruction. Med Phys 2009;36(8):3654–70.
87. Kinahan PE, Vesselle H, MacDonald L, et al. Whole-body respiratory gated PET/CT. J Nucl Med 2006; 47(1):187P.
88. Pan T. Comparison of helical and cine acquisitions for 4D-CT imaging with multislice CT. Med Phys 2005;32(2):627–34.
89. Li T, Thorndyke B, Schreibmann E, et al. Model-based image reconstruction for four-dimensional PET. Med Phys 2006;33(5):1288–98.